Mechanical properties of aluminum, zirconium, hafnium and tantalum oxides and their nanolaminates grown by atomic layer deposition

Taivo Jõgiaas [a,*], Roberts Zabels [b], Aile Tamm [a], Maido Merisalu [a], Irina Hussainova [c], Mikko Heikkilä [d], Hugo Mändar [a], Kaupo Kukli [a,d], Mikko Ritala [d], Markku Leskelä [d]

[a] University of Tartu, Institute of Physics, Department of Materials Science, Ravila 14C, EE-50411 Tartu, Estonia
[b] University of Latvia, Institute of Solid State Physics, Kengaraga str. 8, LV-1063 Riga, Latvia
[c] Tallinn University of Technology, Department of Materials Engineering, Ehitajate tee 5, EE-19086 Tallinn, Estonia
[d] University of Helsinki, Department of Chemistry, P.O. Box 55, FI-00014, Finland

ABSTRACT

The mechanical properties of two different metal oxide nanolaminates comprised of Ta_2O_5 and Al_2O_3, HfO_2 or ZrO_2, grown on soda–lime glass substrate by atomic layer deposition, were investigated. Ta_2O_5 and Al_2O_3 layers were amorphous, whereas ZrO_2 and HfO_2 possessed crystalline structure. Thickness of single oxide layers was varied between 2.5 and 15 nm. The total thickness of the laminate structures was in the range of 160–170 nm. The hardness values of single layer oxides on glass ranged from 6.7 GPa (Ta_2O_5) to 9.5 GPa (Al_2O_3). Corresponding elastic moduli were 96 GPa and 101 GPa. The hardnesses of laminates were in the range of 6.8–7.8 GPa and elastic moduli were between 93 and 118 GPa. The results implied a correlation between mechanical properties and the relative content of constituent single oxides.

© 2015 Elsevier B.V. All rights reserved.

1. Introduction

The microstructural design has attracted a certain interest in the development of hard coatings consisting of a variety of materials ranging from single metal oxides [1–4] to composites or nanolaminates of chemically distinctive compounds [5–8]. Mechanically resistive nanolaminates of different oxides have been deposited by a variety of physical and chemical deposition methods, for example, laser ablation [9], electrophoretic deposition [9], or sputtering [10,11,8] of Al_2O_3–ZrO_2, laser ablation of CeO_2–Gd_2O_3 [12], and atomic layer deposition (ALD) of TiO_2–Al_2O_3 [12–14], Al_2O_3–Ta_2O_5 [15], Al_2O_3–ZnO [17], ZnO/ Al_2O_3/ZrO_2 [18], or aluminum oxide–aluminum alkoxide [3] systems. Moreover, fabrication of metal oxide nanolaminates by chemical vapor deposition (CVD) and atomic layer deposition (ALD) methods allows achieving conformal growth on rough surfaces [14]. Metal oxide laminates have been studied as protective coatings on surfaces of demanding metal alloys, e.g. Al_2O_3–TiO_2 [15] or Al_2O_3–Ta_2O_5 laminates on steel [16]. In nanolaminates, different useful physical properties of constituent material layers can be tailored e.g. crystallinity and higher local density of one component with amorphous and laterally homogeneous, uniformly disordered structure of another component material, accompanied by the repeatedly formed interfaces between constituent layers. Among other potential applications, wear-resistant oxide–metal multilayers deposited on glass have been of interest as hard and stable optical coatings [19,20].

Laminates previously have been mechanically evaluated by three point bending for the flexural strength determination [9], Vickers [13, 14] or Berkovich [9–11] indentation, and steel ball wear tests [18]. In the present study, HfO_2–Ta_2O_5 [20], ZrO_2–Ta_2O_5 [21], and Al_2O_3–Ta_2O_5 [22] nanolaminates grown by ALD on glass substrates were investigated by nanoindentation technique. Indentation tests were conducted using continuous stiffness method [23,24]. In parallel with laminates, single layer oxide samples grown to thicknesses comparable to that of laminates as well as bare glass substrates were tested.

2. Experimental details

Nanolaminates were deposited in a hot-wall flow-type ALD reactor F120 (ASM Microchemistry Ltd.) [25] at 325 °C and at reactor pressure of 10 mbar using water vapor as oxygen source and $Ta(OC_2H_5)_5$, $Al(CH_3)_3$, $HfCl_4$ and $ZrCl_4$ as metal precursors. Precursor pulse lengths were 0.2 s for metal precursors (0.4 s for $HfCl_4$) and 0.5–2.0 s for H_2O. The metal precursors were evaporated from open glass boats inside the reactor. Evaporation temperatures for $HfCl_4$ and $ZrCl4$ were 140 °C

and 150 °C, respectively. Nitrogen was used as the carrier and purging gas with purge lengths of 0.5 s. The substrates used were soda–lime glass with the surface area of 5×5 cm $\times$ cm, cleaned prior to deposition in ethanol and dried in nitrogen flow. The laminates were deposited by alternate layering of two different oxides, varying thickness periods within HfO_2–Ta_2O_5, ZrO_2–Ta_2O_5, and Al_2O_3–Ta_2O_5 double-layers. The number of ALD cycles applied for the growth of a single 2.5–15 nm thick layer constituting a nanolaminate was varied in the range of 50–300. Growth rates of single-oxide interlayers were evaluated from single oxide films grown to the thickness of about 160–170 nm. These growth rates were used in calculating the appropriate number of deposition cycles required to achieve the target thicknesses of the thin single layers in the multi-layer structure. The nominal thicknesses for the constituent layers were estimated, prior to the growth, considering average growth rates of 0.055 nm/cycle for HfO_2 and ZrO_2, 0.06–0.07 nm/cycle for Al_2O_3, and 0.04 nm/cycle for Ta_2O_5 [21,22].

In the following text nanolaminates will be designated via their growth recipes expressed by the nominal thicknesses of the intermittent layers. For example, the sequence written as $10 \times (15\ ZrO_2 + 5\ Ta_2O_5)$ nm denotes 10 double layers of ZrO_2–Ta_2O_5 with each ZrO_2 and Ta_2O_5 single layer grown to thicknesses of 15 and 5 nm, respectively.

The structure and phase compositions of nanolaminates were determined using either Panalytical X'Pert PRO or Rigaku Smartlab X-ray diffractometer in grazing incidence mode with incidence angles between 0.34 and 1°. X-ray reflection patterns (XRR, detector scanning angle 0–3.5°) were also obtained using the same diffractometers. Scanning electron microscopy (SEM) using Helios™ NanoLab 600 (FEI) instrument was employed for imaging the traces of nanoindentation and sample cutting with focused ion beam (FIB). Prior to FIB cutting, magnetron sputtering was used to deposit a protective and conductive layer of platinum. Instrumented nanoindentation was performed by Agilent Nanoindenter G200 using continuous stiffness measurement technique. The area function of the Berkovich diamond tip was calibrated using fused silica as reference. Indentations were performed up to a depth of 1.8 μm. The results were averaged between data obtained from eight locations indented on the surface area of 1×1 cm $\times$ cm, approximately (Fig. 1).

3. Results and discussion

3.1. Film structure

X-ray diffraction (XRD) patterns of single Al_2O_3 and Ta_2O_5 films did not reveal any peaks, verifying the absence of long-range order in these oxides. The Al_2O_3, Ta_2O_5 and also thinner HfO_2 and ZrO_2 films could be considered as X-ray amorphous (the possible crystal size remained below detection limit). The diffraction patterns of ZrO_2–Ta_2O_5 and HfO_2–Ta_2O_5 nanolaminates are depicted in Fig. 2. ZrO_2 and HfO_2 films were nanocrystalline, revealing the formation of structural mixtures of stable monoclinic and metastable cubic or tetragonal phases.

Films containing HfO_2 showed clear characteristic peaks of monoclinic phase but some reflections attributable to the metastable tetragonal phase also appeared. In general, the intensity of the reflections increased with the thickness of ZrO_2 and HfO_2 layers. The peaks in the HfO_2 patterns started to form at layer thicknesses around 10 nm. ZrO_2–Ta_2O_5 nanolaminates showed a presence of the tetragonal/cubic phase of the ZrO_2–Ta_2O_5 nanolaminates, whereas the stable monoclinic phase was not detected. The reflections started to appear at ZrO_2 layer thicknesses of 5 nm. One can also note, that 5 nm may occur at the possible limit to the convenient recognition of crystal growth. Below this value, approximately, the X-ray reflections may remain too wide for their reliable distinction from the background signal and the material, even when a short range order is present, it could then be regarded as X-ray amorphous phase. Nevertheless, such kind of laminates consists of structurally and chemically distinct metal oxide, e.g. ZrO_2 and
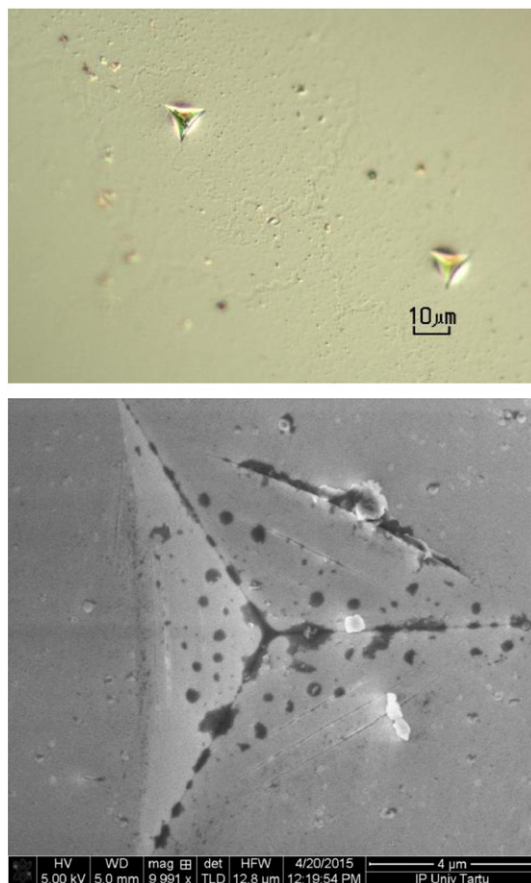
Fig. 1. Optical microscopy (upper panel, the scale bar is 10 μm) and scanning electron microscopy (lower panel, scale bar is 4 μm) images of a triangular Berkovich indenter mark on the surface of the nanolaminate grown with layer sequence of 5 nm $Ta_2O_5 + 33 \times (2.5\ nm\ ZrO_2 + 2.5\ nm\ Ta_2O_5)$.

Ta_2O_5, layers alternately deposited on planar substrates, forming sandwiches with microscopically distinguishable constituent layers.

Visualizing further the growth of nanolaminate structures, a representative X-ray reflectivity pattern, measured at angles from 0 to 3.5°, is depicted in Fig. 3. Similar curves verifying the multilayer structure were recorded for all the nanolaminates. The fitted curve in Fig. 3 is in a good agreement with the nominal thickness sequence of 10 nm $Ta_2O_5 + 8 \times (10\ nm\ HfO_2 + 10\ nm\ Ta_2O_5)$. Stable thicknesses of Ta_2O_5 layers have been fitted between 9.7 and 9.9 nm throughout the laminate. Also the thickness of the HfO_2 layers remained, in practice, constant at 9.0 nm. The roughness of both Ta_2O_5 and HfO_2 layers had a tendency to slightly decrease, looking from the substrate to the outermost surface, from 0.7 to 0.5 nm, and from 0.8 to 0.5 nm, respectively.

For the comparison, XRR analysis of the laminate grown with a nominal thickness sequence of 5 nm $Ta_2O_5 + 8 \times (15\ nm\ HfO_2 + 5\ nm\ Ta_2O_5)$, demonstrating a considerably higher degree of crystallinity (Fig. 2), revealed that the thickness of the Ta_2O_5 layers remained in the range of 6.4–6.9 nm, without a clear systematic change throughout the total laminate thickness. However, a slight change in the HfO_2 thickness occurred, from 14.6 to 15.6 nm counted from the substrate to the surface. Throughout the thickness of the laminate the roughness of HfO_2 layers increased from 0.3 to 1.2 nm, and for Ta_2O_5 layers from 0.4 to 1.4 nm. It could be seen, that the thickness of the constituent layers remained almost constant, i.e. varied in a rather narrow range throughout the thickness of the nanolaminate. A certain development in the roughness of the constituting layers may occur, i.e. roughness can increase towards the top layers of the laminate if the thickness of the crystalline HfO_2 interlayers is sufficient to allow stronger crystallization.